ADVANCED FUNCTIONAL MATERIALS
www.afm-journal.de

Poly(*N*-isopropylacrylamide)-Clay Nanocomposite Hydrogels with Responsive Bending Property as Temperature-Controlled Manipulators

Chen Yao, Zhuang Liu, Chao Yang, Wei Wang, Xiao-Jie Ju, Rui Xie, and Liang-Yin Chu**

Novel poly(*N*-isopropylacrylamide)-clay (PNIPAM-clay) nanocomposite (NC) hydrogels with both excellent responsive bending and elastic properties are developed as temperature-controlled manipulators. The PNIPAM-clay NC structure provides the hydrogel with excellent mechanical property, and the thermoresponsive bending property of the PNIPAM-clay NC hydrogel is achieved by designing an asymmetrical distribution of nanoclays across the hydrogel thickness. The hydrogel is simply fabricated by a two-step photo polymerization. The thermoresponsive bending property of the PNIPAM-clay NC hydrogel is resulted from the unequal forces generated by the thermoinduced asynchronous shrinkage of hydrogel layers with different clay contents. The thermoresponsive bending direction and degree of the PNIPAM-clay NC hydrogel can be adjusted by controlling the thickness ratio of the hydrogel layers with different clay contents. The prepared PNIPAM-clay NC hydrogels exhibit rapid, reversible, and repeatable thermoresponsive bending/unbending characteristics upon heating and cooling. The proposed PNIPAM-clay NC hydrogels with excellent responsive bending property are demonstrated as temperature-controlled manipulators for various applications including encapsulation, capture, and transportation of targeted objects. They are highly attractive material candidates for stimuli-responsive "smart" soft robots in myriad fields such as manipulators, grippers, and cantilever sensors.

1. Introduction

Smart hydrogels with dramatic change of volume or other properties in responding to external stimuli such as mild change in temperature,[1–4] pH,[5–8] humidity,[9–11] special ions or molecules,[12–15] ionic strength or electric field,[16–18] have captured much interests recently. Because of the stimuli-responsive properties, smart hydrogels play an increasingly important role in myriad applications, such as smart actuators for chemical valves,[19] scaffolds for tissue engineering,[20,21] "on/off" switches for chemical reactions,[22,23] vehicles for drug delivery,[20,21,24] matrices for bioseparations,[21,25] as well as artificial "muscles" and soft biomimetic machines.[26–29] The stimuli-responsive deformation movements of smart hydrogels include expansion/contraction and bending/unbending.[6,30] The expansion/contraction is caused by homogeneous swelling/shrinkage of the hydrogels in all directions; while, the bending/unbending is a result of inhomogeneous swelling/shrinkage of the hydrogels with different magnitudes in different directions. The bending/unbending movements of smart hydrogels depend on many parameters such as the hydrogel shape and size, as well as the inhomogeneous architecture.[31] The stimuli-responsive hydrogels, which are able to bend/unbend in response to environmental stimuli, have drawn much attention because they are highly promising in many biomimetic applications such as soft vehicles,[32–35] manipulators,[36–39] and crawlers.[10,40] Among the stimuli-responsive hydrogels, temperature-responsive ones are the most attractive, because temperature variation is very easily controlled as an external stimulus. In many practical applications such as temperature-controlled "soft robots," both significant responsive-bending property and excellent mechanical property are indispensable for the temperature-responsive hydrogels.

Up to now, several kinds of temperature-responsive hydrogels with responsive-bending properties have been developed.[1,41–48] Due to the inhomogeneous internal structure, obvious bending/unbending deformations of hydrogels can be achieved by asymmetrically responding to temperature. Several strategies have been developed to fabricate temperature-responsive hydrogels with inhomogeneous structures by fabricating an asymmetrical distribution of crosslinking degree across the hydrogel or a multilayer structure. The inhomogeneous crosslinking structures of temperature-responsive hydrogels can be generated by controlling the preparation conditions. For example, when the photoirradiation is used to initiate the polymerization of temperature-responsive hydrogels, the photoirradiation time and area can be controlled to produce

C. Yao, Dr. Z. Liu, C. Yang, Dr. W. Wang, Prof. X.-J. Ju, Prof. R. Xie, Prof. L.-Y. Chu
School of Chemical Engineering Sichuan University
Chengdu, Sichuan 610065, P. R. China
E-mail: liuz@scu.edu.cn; chuly@scu.edu.cn
Prof. X.-J. Ju, Prof. L.-Y. Chu
State Key Laboratory of Polymer Materials Engineering
Sichuan University
Chengdu, Sichuan 610065, P. R. China

DOI: 10.1002/adfm.201500420

asymmetrical crosslinking structures.[41–43] Besides, nanoparticles dispersed the hydrogels with an asymmetrical distribution, which is realized by external field, can also generate an inhomogeneous internal structure inside temperature-responsive hydrogels.[44] These strategies can effectively produce the inhomogeneous crosslinking structures of the temperature-responsive hydrogels, but most of the hydrogels are featured with poor mechanical properties because their polymeric networks are chemically crosslinked by small molecules, and the addition of nonresponsive nanoparticles results in poor responsive characteristics of hydrogels. Both poor mechanical properties and poor responsive characteristics severely limit the practical applications of the hydrogels. To improve the mechanical properties of the hydrogels, several strategies have been developed by generating double-network hydrogels consisting of two interpenetrating networks,[49,50] or by using organic/inorganic particles as crosslinkers for synthesizing nanocomposite (NC) hydrogels.[51–55] All the strategies can significantly improve the mechanical properties of hydrogels, but they cannot help to improve the responsive-bending properties. Another strategy for achieving the hydrogels with asymmetrical response to temperature, is to prepare gels with layered structures consisting of a temperature-responsive hydrogel layer and a nonresponsive substrate layer.[1,45–48] Although the mechanical properties of the hydrogels are improved to some extent by adding the nonresponsive substrate layer, the bending degree of the hydrogels is limited due to the nonresponsive layer. Moreover, the hydrogel layers are combined by physical/chemical connection such as semi-interpenetrating network formation[1,45–47] as well as molecular recognition,[48] which may need certain special requirements. In summary, easy fabrication of temperature-responsive hydrogels with both significant responsive bending/unbending properties and excellent mechanical properties still remains a challenge.

In this study, we report on a novel type of poly(*N*-isopropylacrylamide)-clay (PNIPAM-clay) NC hydrogels with both significant responsive bending/unbending properties and excellent mechanical properties as temperature-controlled manipulators. The PNIPAM-clay NC structure provides the hydrogel with excellent elastic property and rapid thermoresponsive property.[52–54] The thermoresponsive bending property of the PNIPAM-clay NC hydrogel is achieved for the first time by designing an asymmetrical distribution of nanoclays across the hydrogel thickness, which is simply achieved by a two-step photopolymerization. The two layers with different clay contents in the PNIPAM-clay NC hydrogels possess different thermoinduced shrinking rates and different thermoinduced mechanical forces;[51–55] as a result, the PNIPAM-clay NC hydrogels exhibit significant thermoinduced bending behaviors. Besides, the volume change of the hydrogels upon thermoresponsive shrinking and swelling in water is beneficial to the proposed hydrogel manipulators, because the thermoinduced volume shrinking and swelling of the PNIPAM-clay NC hydrogels are helpful to the tight capture and easy release of target objects via the thermotriggered bending/unbending. The proposed PNIPAM-clay NC hydrogels with excellent temperature-responsive bending characteristics are demonstrated as temperature-controlled manipulators for various applications such as encapsulation, capture, and transportation of certain target objects in aqueous environments.

2. Results and Discussion

2.1. Strategy for Design and Fabrication of Thermoresponsive Hydrogels with Both Excellent Mechanical and Responsive Bending Properties

In this study, the thermoresponsive bending characteristics of the PNIPAM-clay NC hydrogels are achieved by designing an asymmetrical distribution of nanoclays across the hydrogel thickness (**Figure 1**). It has been reported that the nanocomposite hydrogels prepared with nanoclays as crosslinkers are very elastic and have much better mechanical property than normal hydrogels chemically crosslinked by small molecules.[52–54] For PNIPAM-clay NC hydrogels, the thermoresponsive volume-changing rate of hydrogel decreases with increasing the clay content,[51–54] while the mechanical force caused by the conformational change in PNIPAM networks increases with increasing the clay content.[55] Therefore, the thermoresponsive volume-changing rate and the mechanical force caused by the conformational change of NC hydrogels are different with varying the clay contents. To illustrate the thermoresponsive bending mechanism, the cross-section of a double-layered PNIPAM-clay NC hydrogel with two different contents of clay across the hydrogel thickness is shown in Figure 1, in which "NC3" and "NC5," respectively, represent the clay concentrations in the hydrogels are 3×10^{-2} and 5×10^{-2} mol L^{-1}, and $\sum F_3$ and $\sum F_5$ represent the resultant forces on the NC3 side and NC5 side, respectively. At the beginning ($t = t_0$), when the environmental temperature is lower than the volume phase transition temperature (VPTT) of PNIPAM, the hydrogel strip in water is straight (Figure 1a). Then, when the temperature is rapidly increased from lower to higher than the VPTT ($t = t_1$), the NC3 side shrinks faster and generates a larger resultant force than the NC5 side, which causes the hydrogel strip first bends toward the NC3 side slightly (Figure 1b). Next, the NC5 side starts to shrink ($t = t_2$), and generates a larger resultant force than the NC3 side does ($\sum F_5 > \sum F_3$), because the maximum mechanical force of the PNIPAM-clay NC hydrogel increases with increasing the clay content;[55] as a result, the bending direction of the hydrogel strip reverses and bends toward the NC5 side (Figure 1c). Due to the inertial effect ($t = t_3$), the hydrogel strip can bend very seriously toward the NC5 side (Figure 1d). Finally, the hydrogel strip at the equilibrium state ($t = t_n$) remains unchanged bending shape toward the NC5 side (Figure 1e). Thus, the thermoresponsive hydrogels are featured with both excellent mechanical and responsive bending properties.

The fabrication process of the PNIPAM-clay NC hydrogel designed with an asymmetrical distribution of nanoclays across the hydrogel thickness is schematically illustrated in **Figure 2**. The mold for hydrogel fabrication consists of a polytetrafluoroethylene (PTFE) plate, a thin PTFE frame, and a transparent quartz plate (Figure 2a). When they are clipped together, a square space is formed with adjustable thickness by the PTFE frame. The aqueous solution, which contains monomer

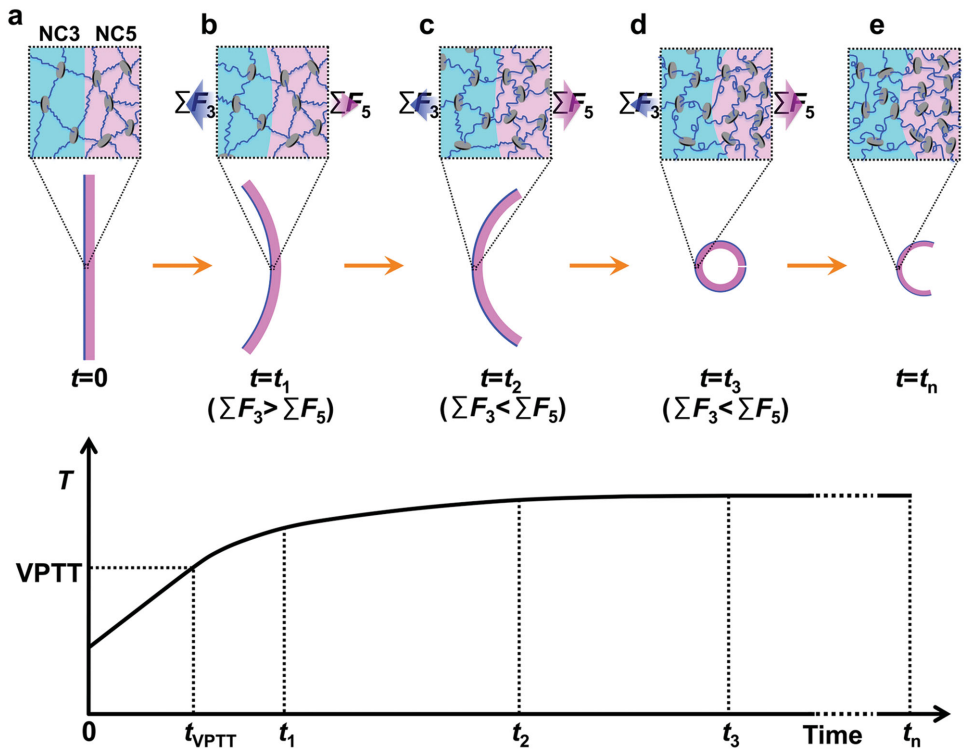

Figure 1. Schematic illustration of the thermoresponsive bending mechanism of the PNIPAM-clay NC hydrogel designed with an asymmetrical distribution of nanoclays across the hydrogel thickness. "NC3" represents the clay concentration in the hydrogel is 3×10^{-2} mol L^{-1}, and "NC5" represents that is 5×10^{-2} mol L^{-1}. "$\sum F_3$" and "$\sum F_5$" represent the resultant forces on the NC3 side and NC5 side, respectively. a) At the beginning ($t = t_0$), the hydrogel strip in water is straight. b) Then, when the temperature is rapidly increased from lower to higher than the VPTT ($t = t_1$), the hydrogel strip in water first bends toward the NC3 side slightly, because the NC3 side shrinks faster than the NC5 side. c) Next, the NC5 side starts to shrink ($t = t_2$), and generates a larger resultant force than the NC3 side does ($\sum F_5 > \sum F_3$); as a result, the bending direction of the hydrogel strip reverses and bends toward the NC5 side. d) Due to the inertial effect ($t = t_3$), the hydrogel strip can bend very seriously toward the NC5 side. e) Finally, the hydrogel strip at the equilibrium state ($t = t_n$) remains unchanged bending shape toward the NC5 side.

(*N*-isopropylacrylamide, NIPAM), clay (Laponite XLG), dye (Rhodamine B), and photoinitiator (1-hydroxy-cyclohexyl-phenylketone, Irg. 184), is injected into the assembled mold (Figure 2b), and then UV irradiation is carried out for 3 min from the quartz plate side to initiate the polymerization in an ice-water bath (Figure 2c). After removing the PTFE plate and frame away, monolayer NC hydrogel is left on the quartz plate (Figure 2d) and can be obtained as product after releasing from the quartz plate (Figure 2e). To obtain double-layered NC hydrogel with an asymmetrical distribution of nanoclays across the hydrogel thickness, the PTFE frame is replaced by a thicker one (Figure 2f), in which the thickness of "frame-2" is thicker than that of "frame-1." Then, another aqueous solution, which contains monomer NIPAM with the same concentration, Laponite XLG with different concentrations, another dye (methylene blue), and photoinitiator Irg. 184, is injected into the new space inside the reassembled mold (Figure 2g). Next, UV irradiation is carried out for 5 min from the quartz plate side to initiate the polymerization again in an ice-water bath (Figure 2h). Finally, the designed double-layered NC hydrogel is obtained after releasing from the mold (Figure 2i). The thickness of the NC hydrogel layer depends on the thickness of PTFE frame, while the composition of the NC hydrogel layer is controlled by the injection solution. The obtained double-layered NC hydrogel with an asymmetrical distribution of nanoclays across the hydrogel thickness is washed thoroughly with water for several days to remove the unreacted chemicals. The prepared PNIPAM-clay NC hydrogel is coded as "NC*i*-NC*j*-α," in which "*i*" and "*j*" represent the clay concentrations of the first layer and the second layer, respectively, and "α" is the thickness ratio of the first layer to the second layer after completely swelling in water. For example, a hydrogel code "NC5–NC3-4.33" denotes that, the clay concentrations of the first layer and the second layer are 5×10^{-2} and 3×10^{-2} mol L^{-1}, respectively, and the thickness ratio of the NC5 layer to the NC3 layer after completely swelling is 4.33. As expected, the results of mechanical tensile strain–stress experiments show that the PNIPAM-clay NC hydrogels have excellent mechanical properties with large tensile strain at break and high tensile strength (Figures S1 and S2, Supporting Information), which are consistent with those reported in literatures.[52–54]

2.2. Morphological Analyses of PNIPAM-Clay NC Hydrogels

Optical micrographs of NC5 hydrogel and NC5–NC3-4.33 hydrogel just released from the mold and at equilibrium swelling states in water at room temperature are shown in **Figure 3**, in which "h_3" and "h_5" represent the thicknesses

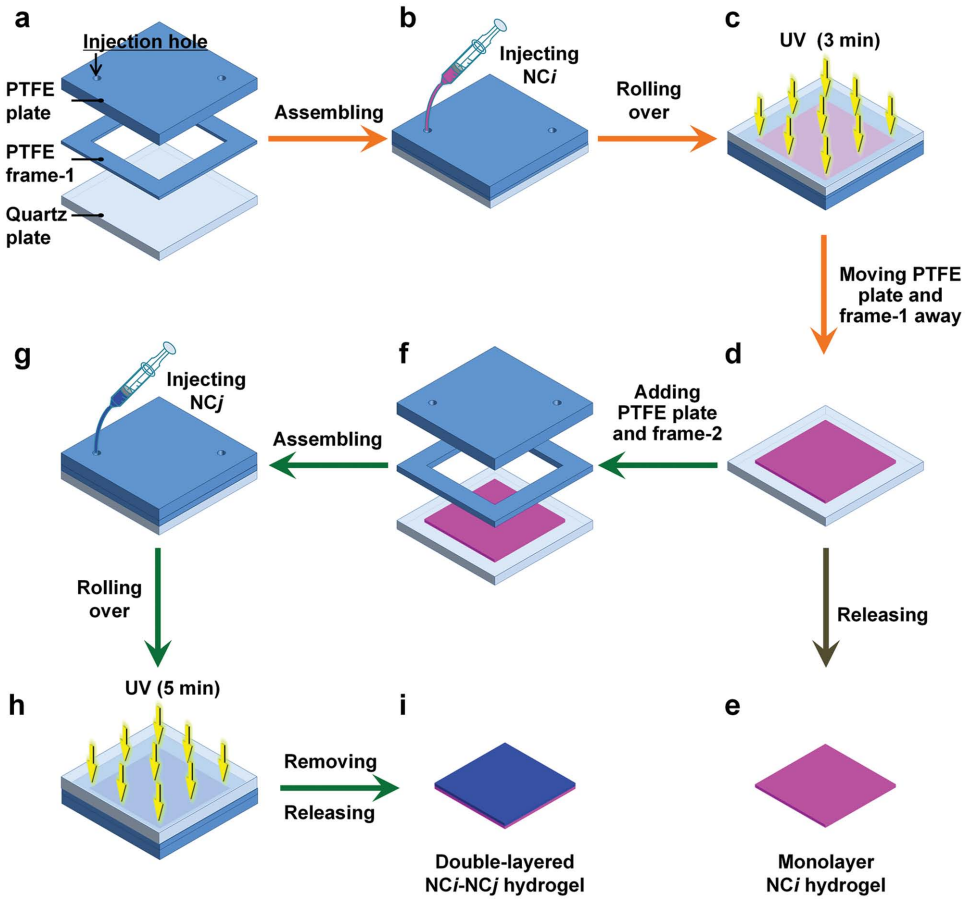

Figure 2. Schematic illustration of the fabrication process of the PNIPAM-clay NC hydrogel designed with an asymmetrical distribution of nanoclays across the hydrogel thickness. a) The mold for hydrogel fabrication consists of a polytetrafluoroethylene (PTFE) plate, a thin PTFE frame, and a transparent quartz plate. b) The aqueous solution, which contains monomer, clay, dye (red), and photoinitiator, is injected into the assembled mold, and c) then UV irradiation is carried out for 3 min from the quartz plate side to initiate the polymerization. d) After removing the PTFE plate and frame away, monolayer NC hydrogel is left on the quartz plate and e) can be obtained as product after releasing from the quartz plate. f) To obtain double-layered NC hydrogel with an asymmetrical distribution of nanoclays across the hydrogel thickness, the PTFE frame is replaced by a thicker one, in which the thickness of "frame-2" is thicker than that of "frame-1." g) Then, another aqueous solution, which contains monomer, clay with different concentrations, another dye (blue), and photoinitiator, is injected into the new space inside the reassembled mold. h) Next, UV irradiation is carried out for 5 min from the quartz plate side to initiate the polymerization. i) Finally, the designed double-layered NC hydrogel is obtained after releasing from the mold.

of NC3 hydrogel and NC5 hydrogel, respectively. The NC5 hydrogel is dyed by Rhodamine B, while the NC3 hydrogel is dyed by methylene blue. Both the NC5 hydrogel and NC5–NC3-4.33 hydrogel are uniform and transparent, and it is obvious that the NC3 and NC5 layers still combine very well after swelling to the equilibrium state.

In order to investigate the combination of the NC5 and NC3 hydrogel layers, the PNIPAM-clay network structures of the hydrogels are observed by scanning electron microscope (SEM). The SEM images of the microstructures of freeze-dried NC5–NC3 hydrogels are shown in **Figure 4**. The freeze-dried NC5–NC3 hydrogel shows honeycomb-like structure with nearly dense cell walls (Figure 4a). The internal NC3 layer (Figure 4b) and NC5 layer (Figure 4c) exhibit a uniform porous network. Because the hydrogel samples are freeze-dried for SEM observation, the honeycomb-like microporous structures within the hydrogels after freeze-drying are resulted from the ice crystals present in the swollen hydrogels acting as templates for pore generation.[56] Such micropores in the freeze-dried hydrogels do not have remarkable influences on the bending performances of hydrogels. At the interface, plenty of crosslinks are formed across the interface due to the interactions of the polymer chains and neighboring clay platelets by hydrogen bonding, which lock the two layers of the NC5–NC3 hydrogel together tightly (Figure 4d). Although there exists an interface between the two layers in the NC5–NC3 hydrogel, the two layers do not separate but still combine very tightly even after ten bending/unbending cycles (Figure S3, Supporting Information).

2.3. Thermoresponsive Volume Change and Mechanical Characteristics of PNIPAM-Clay NC Hydrogels

Effects of clay concentrations in NC hydrogels on the equilibrium thermoresponsive volume phase transition characteristics of monolayer NC hydrogels with different thicknesses are shown in **Figure 5**. The thicknesses of monolayer NC hydrogels at the equilibrium swelling states in water at room temperature

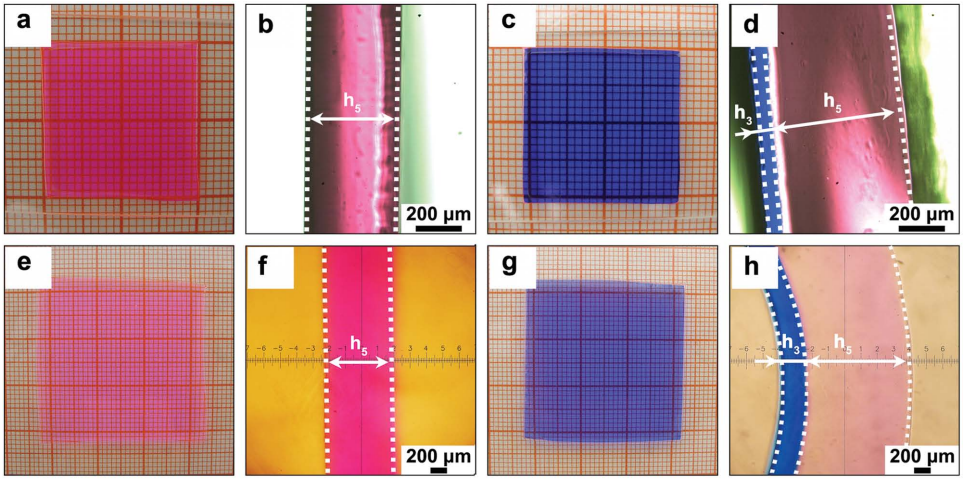

Figure 3. Optical micrographs of a,b,e,f) NC5 hydrogel and c,d,g,h) NC5–NC3-4.33 hydrogel a–d) just released from the mold and e–h) at equilibrium swelling states in water at room temperature. "h_3" and "h_5" represent the thicknesses of NC3 hydrogel and NC5 hydrogel, respectively.

are directly dependent on the thicknesses of PTFE frames (Figure 5a). The thicknesses of the NC*i* (i = 2, 3, 5) hydrogels at the equilibrium swelling states in water at room temperature, prepared with a PTFE frame thickness of 0.5 mm, are about 0.95 mm. The monolayer NC hydrogels with different thicknesses can be prepared easily by changing the thickness of the PEFT frame. A suffix "[*x*]" is added to the code of the NC*i* hydrogel when the hydrogel prepared by using a PTFE frame with thickness of "*x*" mm. The VPTT values of the NC hydrogels with different clay concentrations and thicknesses are all around 33 °C (Figure 5b). That is, the equilibrium thermoresponsive volume phase transition characteristics of NC hydrogels are not remarkably affected by the clay concentration or the hydrogel thickness.

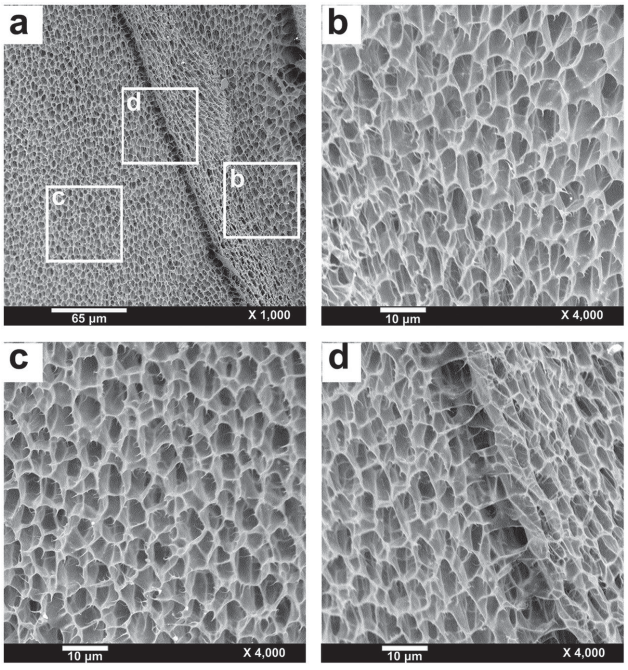

Figure 4. SEM images of a) NC5–NC3 hydrogel, and b) magnified micrographs of NC3 hydrogel, c) NC5 hydrogel and d) the interface between them.

Effects of hydrogel thickness and clay content on the dynamic thermoresponsive volume shrinking characteristics of monolayer NC hydrogels in water with increasing temperature rapidly from 24 to 40 °C are illustrated in **Figure 6**. The "volume ratio" of a hydrogel in the *Y*-axis is the ratio of the hydrogel volume at a certain time to its initial volume, which reflects the shrinking degree of the NC hydrogels. As mentioned above, the thicknesses of monolayer NC hydrogels at the equilibrium swelling states in water at room temperature are directly dependent on the thicknesses of PTFE frames (Figure 5a). In the hydrogel code "NC*i*[*x*]," the symbol "*i*" represents the clay concentration in the hydrogel and "*x*" represents the thickness of the PTFE frame for preparing the hydrogel, e.g., the code "NC3[0.3]" represents a hydrogel with clay concentration of 3×10^{-2} mol L^{-1} and prepared by using a PTFE frame with thickness of 0.3 mm. The results show that, the thinner the NC hydrogel is, the faster the thermotriggered volume shrinkage of the NC hydrogel (Figure 6a), which is resulted from the dimensional effect on the dynamic responsive characteristics.[57] With increasing the clay concentration in the NC hydrogel, the thermotriggered volume shrinkage of the NC hydrogel becomes slightly slower (Figure 6b), which is due to the nonresponsiveness of the nanoclay additives.

The thermoresponsive shrinking and mechanical characteristics of monolayer NC hydrogels with different clay contents play an important role in temperature-triggered asymmetric response of PNIPAM-clay NC hydrogel with an asymmetrical distribution of nanoclays. **Figure 7** shows the thermoresponsive shrinking and mechanical characteristics of NC3 hydrogel and NC5 hydrogel in water. The NC3 and NC5 hydrogels are prepared with uniform thickness but different clay concentrations, and the NC hydrogels are placed into a cuboid container with both ends fixed by clamps. "L_3" and "L_5" denote the lengths of NC3 hydrogel and NC5 hydrogel, respectively. The environmental temperature is increased rapidly from 24 to 39 °C. When the NC3 and NC5 hydrogels are unconnected (Figure 7a–c), both NC5 and NC3 hydrogels shrink with increasing the

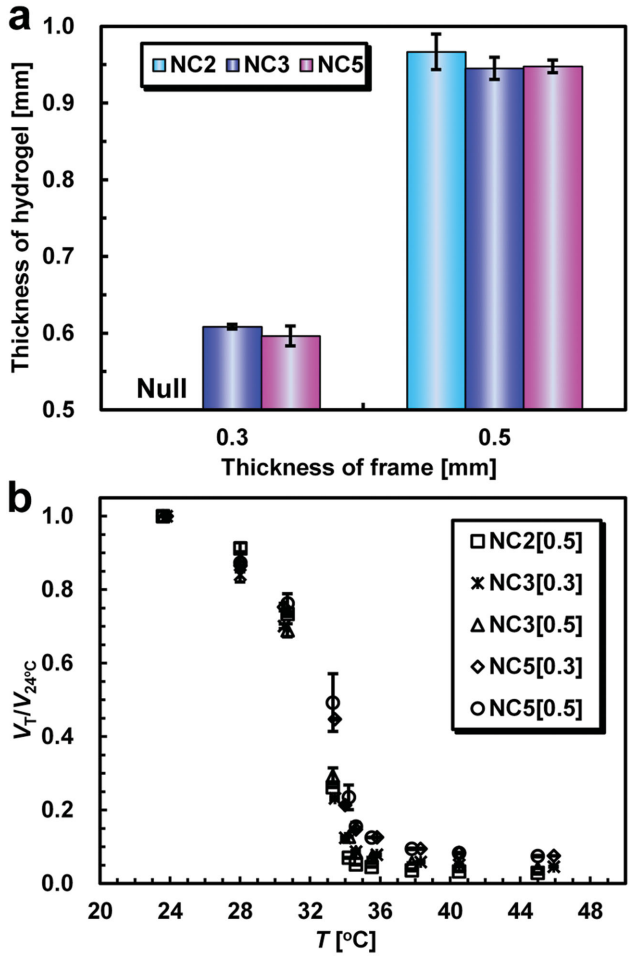

Figure 5. a) Relationship between the thicknesses of PTFE frames and the thicknesses of monolayer NC hydrogels at the equilibrium swelling states in water at room temperature. b) Effects of clay concentrations in NC hydrogels on the equilibrium thermoresponsive volume phase transition characteristics of monolayer NC hydrogels with different thicknesses. "V_T" and "$V_{24\ °C}$" represent the hydrogel volumes at T °C and 24 °C, respectively. In the hydrogel code "NC*i*[*x*]," "*i*" represents the clay concentration in the hydrogel and "*x*" represents the thickness of the PTFE frame for preparing the hydrogel, e.g., the code "NC3[0.3]" represents a hydrogel with clay concentration of 3×10^{-2} mol L^{-1} and prepared by using a PTFE frame with thickness of 0.3 mm.

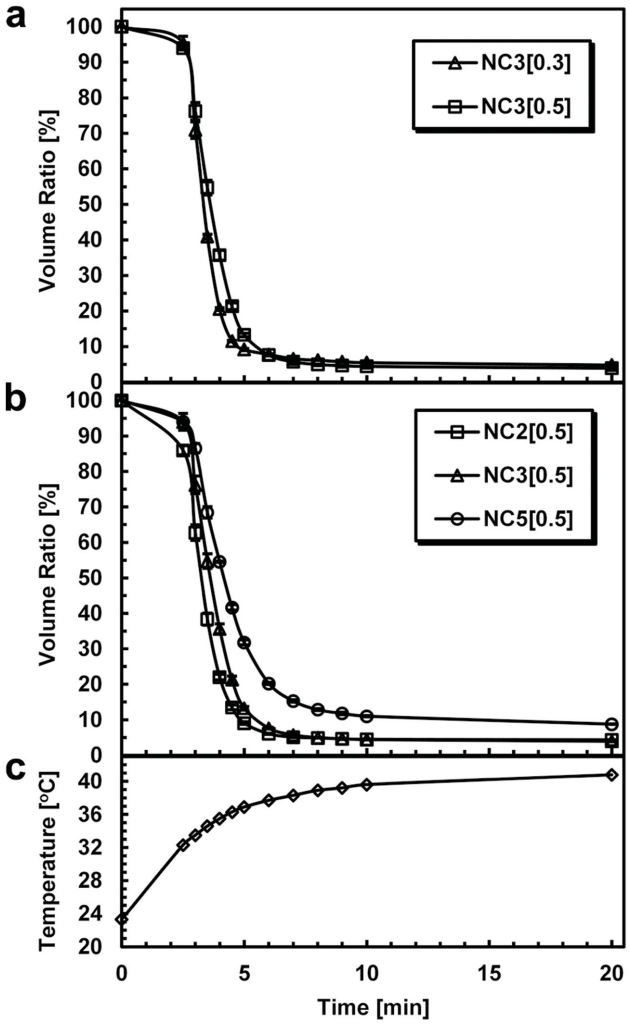

Figure 6. Effects of a) hydrogel thickness and b) clay content on the dynamic thermoresponsive volume shrinking characteristics of monolayer NC hydrogels in water with increasing temperature rapidly from 24 to 40 °C c). The "volume ratio" of a hydrogel in the *Y*-axis is the ratio of the hydrogel volume at a certain time to its initial volume. In the hydrogel code "NC*i*[*x*]," the symbol "*i*" represents the clay concentration in the hydrogel and "*x*" represents the thickness of the PTFE frame for preparing the hydrogel, e.g., the code "NC3[0.3]" represents a hydrogel with clay concentration of 3×10^{-2} mol L^{-1} and prepared by using a PTFE frame with thickness of 0.3 mm.

temperature, and NC3 hydrogel shrinks faster than NC5 hydrogel because less nonresponsive nanoclay additives are existed in NC3 hydrogel. The slight bending of NC5 hydrogel during shrinking process (Figure 7b) is due to the fixing with a clamp. The NC5 hydrogel may be not clamped exactly vertical to the clamp; as a result, when the NC5 hydrogel is shrinking, the thermoinduced mechanical forces are unbalanced in the hydrogels fixed by clamps, and thus the NC5 hydrogel bends slightly while the length change. As references, the free NC hydrogels in water, which are not fixed by clamps, do not bend remarkably while shrinking (Figure S4, Supporting Information). On the contrary, when the NC3 and NC5 hydrogels are connected together (Figure 7d–f), NC3 hydrogel becomes longer and longer while NC5 hydrogel becomes shorter and shorter with increasing the temperature, just like that they are playing a game of tug-of-war, which demonstrates that the NC5 side generates a larger resultant force than the NC3 side does ($\sum F_5 > \sum F_3$) during the thermoinduced shrinking process.

2.4. Thermoresponsive Bending Characteristics of NC5–NC3-α Hydrogels

To investigate the thermoresponsive bending characteristics of NC hydrogels with an asymmetrical distribution of nanoclays across the hydrogel thickness, a series of NC5–NC3-α hydrogels with different thickness ratios are prepared. Effects of the thickness ratio of NC5 layer to NC3 layer (α) on the dynamic thermoresponsive bending and shrinking behaviors of NC5–NC3-α

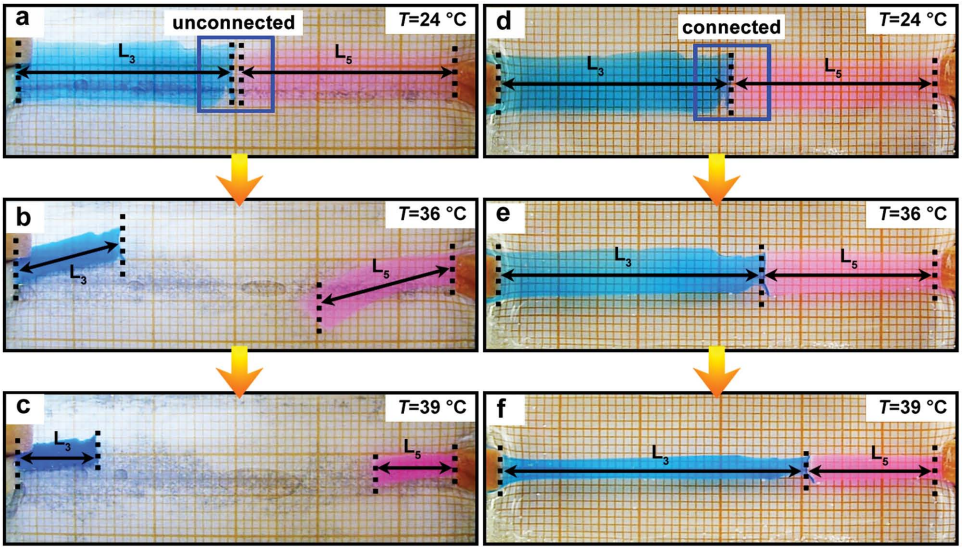

Figure 7. Thermoinduced shrinking and mechanical characteristics of NC3 hydrogel and NC5 hydrogel in water. a–c) When the NC3 and NC5 hydrogels are unconnected, NC3 hydrogel shrinks faster than NC5 hydrogel. d–f) On the contrary, when the NC3 and NC5 hydrogels are connected, NC3 hydrogel becomes longer and longer while NC5 hydrogel becomes shorter and shorter, just like that they are playing a game of tug-of-war, which demonstrates that the NC5 side generates a larger resultant force than the NC3 side does ($\sum F_5 > \sum F_3$). "L_3" and "L_5" denote the lengths of NC3 hydrogel and NC5 hydrogel, respectively.

hydrogel strips in water with increasing temperature rapidly from 20 to 40 °C are shown in **Figure 8**. The NC5–NC3-α hydrogels are all cut into strips with length of 1.5 cm and put in quartz cells, which are full of deionized water and sealed by cover glasses. The ambient temperature of NC5–NC3-α hydrogels at different time intervals is timely measured by a thermocouple. As shown in Figure 8a, the NC5–NC3-1.36 hydrogel strip in water bends toward the NC3 side in deionized water at 20 °C due to the different swelling properties of the NC5 and NC3 hydrogel layers. With increasing temperature from 20 to 40 °C, the NC5–NC3-1.36 hydrogel strip gradually bends to a semicircle at the beginning (within 4 min). Because the NC3 hydrogel shrinks faster than the NC5 hydrogel, the NC5–NC3-1.36 hydrogel strip bends toward the NC3 side. Then, the bending degree of the NC5–NC3-1.36 hydrogel strip becomes less and less with increasing the temperature. Because the NC5 hydrogel shrinks slower than the NC3 hydrogel, the NC5 hydrogel still shrinks further when the NC3 hydrogel reaches the equilibrium state. Because the thickness of NC5 layer is not thick enough, the force caused by the shrinkage of the NC5 layer cannot make the hydrogel strip bending toward the NC5 side. When the value of thickness ratio α increases to 4.33, the hydrogel strip in water bends toward the NC3 side slightly in the first 2 min. With increasing the temperature further, the NC5–NC3-4.33 strip becomes straight subsequently and then bends slightly toward the NC5 side finally. With increasing the value of thickness ratio α further to 8.67, the NC5–NC3-8.67 hydrogel strip in water is almost straight at the beginning at 20 °C. With increasing temperature rapidly from 20 to 40 °C, the NC5–NC3-8.67 hydrogel strip bends rapidly toward the NC5 side. The proposed two-layer PNIPAM-clay hydrogels in this work are featured with rapid responsive rate, and the NC5–NC3-8.67 hydrogel strip bends to equilibrium state in water upon heating from 20 to 40 °C within 5 min. Due to the inertial effect, the hydrogel strip bends very seriously toward the NC5 side to form a circle within 4 min. Finally, the hydrogel strip at the equilibrium state remains unchanged bending shape toward the NC5 side. The results show that the thermoresponsive bending property of NC5–NC3-α hydrogels is decided by the unsymmetrical distribution of nanoclays, and the thermoresponsive bending degree depends on the thickness ratio α of the NC5–NC3 hydrogels.

With increasing the temperature rapidly from 20 to 40 °C, the dynamic thermoresponsive curvature and relative length of the NC5–NC3-α hydrogel strips in water are shown in Figure 8b–d. The curvature value reflects the bending degree. The larger the curvature value is, the higher the bending degree of the hydrogel strip. When the hydrogel strip is straight, the value of curvature is zero. The curvature values can reflect the bending rate, the equilibrium state, and the bending directions of the strips. The dynamic thermoresponsive curvatures of NC5–NC3-1.36, NC5–NC3-4.33, and NC5–NC3-8.67 in water are shown in Figure 8b. When the curvature value in the curve reaches to zero, it is the critical point where the bending direction of the hydrogel strip reverses from NC3 side to NC5 side. The results show that the NC5–NC3-1.36 strip does not change its bending direction, while the NC5–NC3-8.67 and NC5–NC3-4.33 strips do reverse their bending direction as illustrated in Figure 1b. The final bending degrees of the NC5–NC3-1.36 hydrogel strip and NC5–NC3-4.33 hydrogel strip are only 0.15 and 0.08 mm^{-1}, respectively. The equilibrium curvature of NC5–NC3-8.67 hydrogel strip is as large as 0.65 mm^{-1}, which could be large enough for meeting the requirement of thermoresponsive soft manipulators. The dynamic thermoresponsive relative length is the ratio of the length of hydrogel strip at certain time to its initial length, which is shown in Figure 8c. The relative length of the hydrogel strips decreases quickly with increasing temperature. The smaller the α value is, the faster

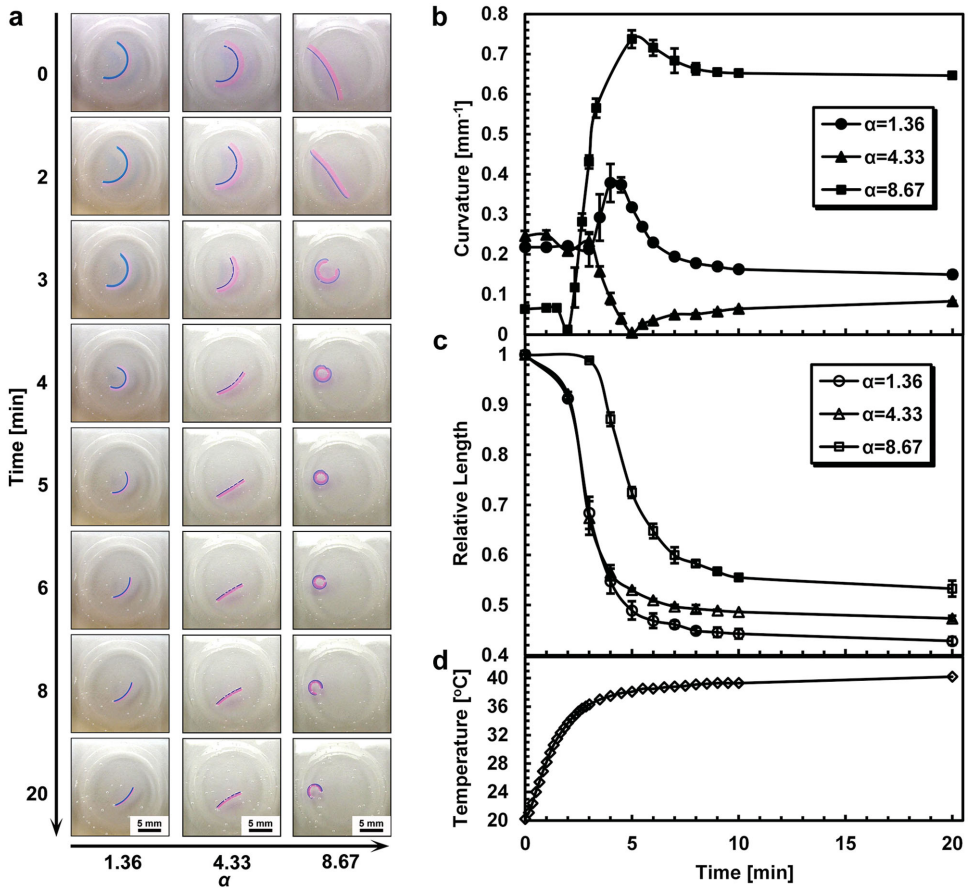

Figure 8. Effects of the thickness ratio of NC5 layer to NC3 layer (α) on the dynamic thermoresponsive bending and shrinking behaviors of NC5–NC3-α hydrogel strips in water with increasing temperature rapidly from 20 to 40 °C. a) Optical photographs of the dynamic processes. b) Dynamic changes of the curvature values of NC5–NC3-α hydrogel strips with different α values. c) Dynamic changes of the relative lengths of NC5–NC3-α hydrogel strips with different α values. d) The corresponding temperature–time curve during the heating process.

the relative length decreases. For capturing substances by the hydrogel, larger bending degree and longer relative length should be better. Therefore, in the subsequent experiments, the α value of NC5–NC3-α hydrogel is selected as 8.67 to achieve remarkable thermoresponsive bending characteristics.

The thermoresponsive bending/unbending and shrinking/swelling behaviors of NC5–NC3-8.67 hydrogel strips in water with switching temperature rapidly between 25 and 40 °C are rapid, reversible, and repeatable (**Figure 9**). The NC5–NC3-8.67 hydrogel strip exhibits a repeatable thermoresponsive bending property in responding to temperature change in four heating–cooling cycles (Figure 9a). When the curvature value of NC5–NC3-8.67 hydrogel strip increases, the relative length decreases in each cycle (Figure 9b–d). After two heating–cooling cycles, the curvature and the relative length of the NC5–NC3-8.67 hydrogel strip become steady.

2.5. Demonstrations of NC5–NC3-8.67 Hydrogels as Temperature-Controlled Manipulators

Figure 10 shows several demonstrations of NC5–NC3-8.67 hydrogels as temperature-controlled manipulators. NC5–NC3-8.67 hydrogel sheets are cut into different shapes for encapsulating and capturing substances as soft manipulators. First, five pieces of hydrogels are cut with rectangular shapes for encapsulation of plastic beads. The rectangular NC5–NC3-8.67 hydrogel sheets are put in the deionized water, and plastic beads are put onto the hydrogels. When the temperature is increased from 30 to 45 °C in 210 s, all the hydrogel sheets bend toward the NC5 side and roll into hydrogel tubes, and thus plastic beads are encapsulated (Figure 10a, see Movie S1, Supporting Information).

Then, cross-shaped NC5–NC3-8.67 hydrogel sheets are prepared to encapsulate substances. With increasing the temperature from 30 to 45 °C in 210 s, the bended cross-shaped hydrogel sheets look like flowers with four petals, which are efficient for encapsulating PTFE pieces (Figure 10b, see Movie S2, Supporting Information).

Next, cross-shaped NC5–NC3-8.67 hydrogel sheets are designed to be transferred by a moving substance or to transfer substance by moving the hydrogel sheet. Figure 10c demonstrates the process of transferring a cross-shaped NC5–NC3-8.67 hydrogel sheet by a moving pearl, just like fishing (see Movie S3, Supporting Information). As mentioned in Figure 1b, when the temperature is rapidly increased from lower to higher

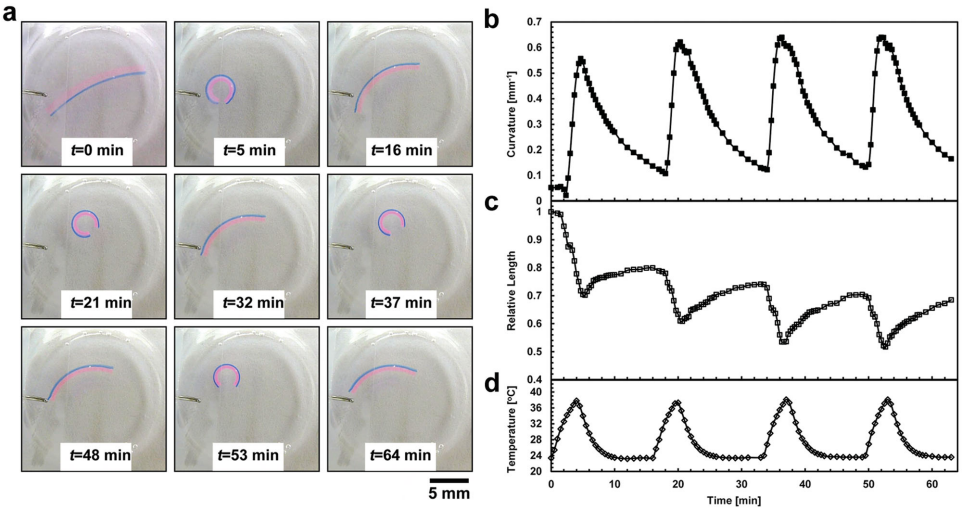

Figure 9. Repeatable thermoresponsive bending/unbending and shrinking/swelling behaviors of NC5–NC3-8.67 hydrogel strips in water with switching temperature rapidly between 25 and 40 °C. a) Optical photographs of the thermoresponsive bending/unbending and shrinking/swelling processes. b) Thermoresponsive change of the curvature of NC5–NC3-8.67 hydrogel strip. c) Thermoresponsive change of the relative length of NC5–NC3-8.67 hydrogel strip. d) The corresponding temperature–time curve during the heating–cooling cycles.

than the VPTT ($t = t_1$), the NC5–NC3 hydrogel first bends toward the NC3 side slightly, because the NC3 side shrinks faster and generates a larger resultant force than the NC5 side. As a result, in cases in Figure 10c1,c2, the hydrogel bends toward NC3 side. With further increasing temperature quickly from 30 to 45 °C, the cross-shaped hydrogel sheet captures the pearl connected to a string and moves with the pearl (Figure 10c3–c5). The pearl is wrapped by the cross-shaped hydrogel tightly. In reverse, a moving cross-shaped NC5–NC3-8.67 hydrogel sheet is designed as a gripper to transfer a PTFE block in water (Figure 10d, see Movie S4, Supporting Information). The hydrogel manipulator is connected to a string with two pieces of thin magnetic sheet, and is used to pick up and transfer the target objects. The manipulator is fully unfolded in water at 20 °C. The PTFE block is put in a water bath at 45 °C. When the hydrogel manipulator is transferred onto the PTFE block in the water bath at 45 °C, it bends rapidly toward the NC5 side and clamps onto the PTFE block. When the hydrogel manipulator is transferred into the water bath at 20 °C, it unfolds and releases the PTFE block. The volume change of the hydrogels upon shrinking and swelling is beneficial to the hydrogel manipulators, because the thermoinduced volume shrinking and swelling of the hydrogels are helpful to the tight capture and easy release of target objects via the thermotriggered bending/unbending. The thermotriggered capture and release behaviors of the hydrogel manipulator, just like the grasp and release actions of human hand, are simply controlled by the temperature change.

3. Conclusion

In summary, poly(*N*-isopropylacrylamide)-clay nanocomposite hydrogels with both excellent responsive bending property and outstanding elastic property have been developed as temperature-controlled manipulators for the first time by designing an asymmetrical distribution of nanoclays across the hydrogel thickness. The thermoresponsive bending property of the NC5–NC3 hydrogel is resulted from the unequal forces generated by asynchronous thermoinduced shrinkage of hydrogel layers with different contents of clay. The thermoresponsive bending degree of NC5–NC3 hydrogels depends on the thickness ratio of the NC5 layer to NC3 layer in the hydrogels. The prepared NC5–NC3-8.67 hydrogels exhibit rapid, reversible, and repeatable thermoresponsive bending/unbending characteristics. The proposed hydrogels with responsive bending property can be designed as soft robots such as manipulators, grippers, as well as cantilever sensors, which are highly attractive and promising in many applications for encapsulating, grapping, and transporting target objects in aqueous environments.

4. Experimental Section

Materials: *N*-isopropylacrylamide (NIPAM), purified by recrystallization, was purchased from Sigma-Aldrich. 1-Hydroxy-cyclohexyl-phenylketone (Irg.184) was purchased from TCI. The synthetic hectorite "Laponite XLG" ($[Mg_{5.34}Li_{0.66}Si_8O_{20}(OH)_4]Na_{0.66}$) was purchased from Rockwood, and used as the inorganic clay after drying at 130 °C for 4 h. Methanol was purchased from Chengdu Kelong Chemicals. Methylene blue was purchased from Tianjin Bodi Chemicals, and Rhodamine B was purchased from Shanghai Chemical Regents. All other reagents were of analytical grade and used without further purification. Deionized water (18.2 MΩ at 25 °C) from a Milli-Q Plus water purification system (Millipore) was used throughout the experiments.

Preparation of Monolayer NC Hydrogels: Uniform aqueous solution containing clay (Laponite XLG), monomer (NIPAM), dyestuff (methylene blue or Rhodamine B), and photoinitiator (Irg.184) was prepared. The dyestuff was first dispersed in water and stirred for about 10 min, and then the clay was added into the dyestuff solution and stirred for 4 h. Subsequently, monomer NIPAM was added into the dyestuff and clay suspension, which was degassed and nitrogen-saturated beforehand under continuous and vigorous stirring in an ice-water bath for another 2 h. The concentration of clay varied in the range from 2×10^{-2} to 5×10^{-2} mol L^{-1}, while the monomer concentration was fixed at

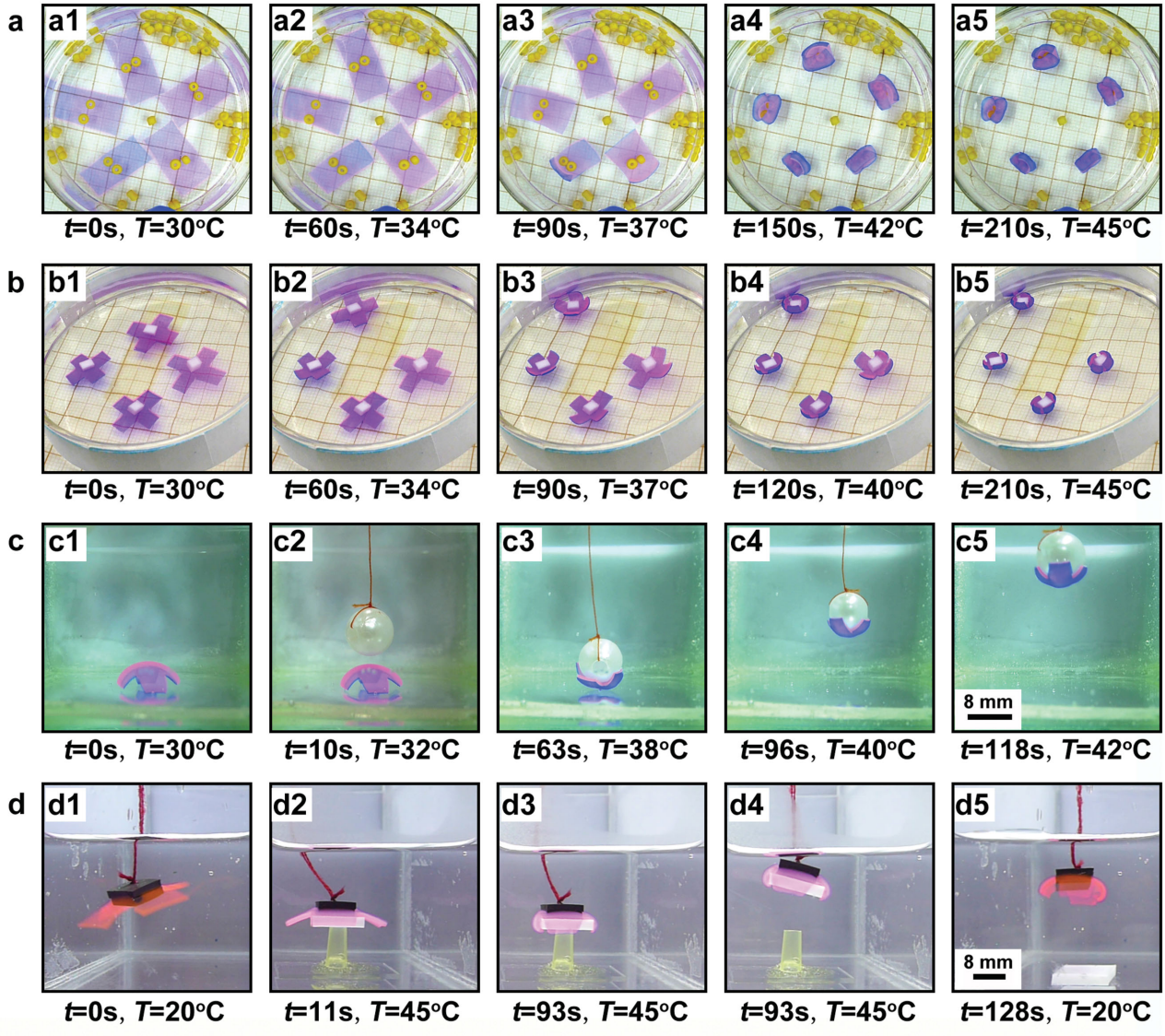

Figure 10. Demonstrations of NC5–NC3-8.67 hydrogels as temperature-controlled manipulators. a) Encapsulation of plastic beads in rectangular NC5–NC3-8.67 hydrogel sheets. b) Encapsulation of PTFE pieces in cross-shaped NC5–NC3-8.67 hydrogel sheets. c) Transportation of a cross-shaped NC5–NC3-8.67 hydrogel sheet by a moving pearl, just like fishing. d) Capture and transportation of a PTFE block by a moving cross-shaped NC5–NC3-8.67 hydrogel sheet as gripper.

1.0 mol L^{-1}. The concentration of dyestuff (methylene blue or Rhodamine B) was fixed at 0.2 g L^{-1}. The concentration ratio of photoinitiator (Irg.184) to monomer (PNIPAM) was fixed at 0.2 wt%. As a typical example, to prepare a NC5[0.5] hydrogel, a transparent aqueous solution with clay concentration of 5×10^{-2} mol L^{-1} consisting of deionized water (10 mL), clay (0.3808 g), and NIPAM (1.13 g) was prepared. Then, Irg.184 (2.26 mg) was added with a methanol solution (100 μL) to the former solution in ice-water bath with stirring. The aqueous reaction mixture was injected into a mold of 50 mm × 50 mm × 0.5 mm, which consisted of a PTFE plate, a transparent quartz plate, and a PTFE spacer of 0.5 mm thickness, and then irradiated under UV light (365 nm) for 3 min in an ice-water bath. The prepared NC5[0.5] hydrogel was purified with excessive water thoroughly.

Preparation of Double-Layered NC Hydrogels: First, a NC5[0.5] hydrogel was prepared according to the procedure mentioned above, and left on the quartz plate. Then, the PTFE frame was replaced by a thicker one, to form a new space between the NC5 hydrogel and PTFE plate after the mold was clipped together (Figure 2f). The aqueous reaction mixture with clay concentration of 3×10^{-2} mol L^{-1} was injected into the new space in the mold. After UV irradiation at 365 nm from the glass side for 5 min in ice-water bath, NC5–NC3 hydrogel was obtained. The prepared NC5–NC3 hydrogel was purified thoroughly with excessive water.

SEM Characterization of NC5–NC3 Hydrogel: The microstructures of freeze-dried NC5–NC3 hydrogels were observed by SEM (G2 Pro, Phenom). The double-layered NC hydrogel samples in deionized water were frozen in liquid nitrogen for 10 min and then lyophilized by a freeze drier (FD-1C-50, Beijing BoYiKang) at −35 °C for about 24 h.

Thermoresponsive Equilibrium Volume Change of Monolayer NC Hydrogels: The monolayer NC hydrogel sheets were cut into the same size (1 cm × 1 cm) and placed in transparent quartz holders, which can be sealed with glass cover by high vacuum grease. The thermoresponsive volume change behaviors of the monolayer NC hydrogels were recorded by a digital camera. The ambient temperature of the monolayer NC hydrogels was controlled by a thermostatic stage

system (TS62, Instec). Before each measurement, the monolayer NC hydrogels at each predetermined temperature had been kept for more than 30 min to reach the equilibrium state. The ambient temperature of the monolayer NC hydrogels at different time intervals was timely measured by a thermocouple.

Dynamic Thermoresponsive Shrinking Behaviors of Monolayer NC Hydrogels: The monolayer NC hydrogel sheets (1 cm × 1 cm) were placed in transparent quartz holders and sealed with glass cover by high vacuum grease, which were placed on a heating stage (TS62, Instec). The ambient temperature of the monolayer NC hydrogels was controlled by the thermostatic stage system. Before the dynamic shrinking experiments, the monolayer NC hydrogels had been equilibrated at 25 °C for more than 30 min to reach a full swelling state. The sudden heating operations were simply achieved by promptly changing the temperature from 25 to 50 °C. The ambient temperature of the monolayer NC hydrogels at different time intervals was timely measured by a thermocouple. The whole dynamic shrinking process was recorded by a digital camera equipped on the top of the quartz holder. Several monolayer NC hydrogel sheets with the same structures were measured to obtain statistic data for the thermoresponsive volume change characteristics.

Dynamic Thermoresponsive Bending Behaviors of NC5–NC3-α Hydrogels: The NC5–NC3-α hydrogels with different α values were all cut into strips of 1.5 cm in length and 0.15 cm in width. The NC5–NC3-α hydrogels were put in transparent quartz holders with pure water, which were placed on a heating stage (TS62, Instec). Before the dynamic shrinking experiments, the double-layered NC hydrogel strips had been equilibrated at 25 °C for more than 30 min to reach the full swelling state. The heating operations were simply achieved by rapidly changing the temperature from 25 to 50 °C with the thermostatic stage system. The ambient temperature of NC5–NC3-α hydrogels at different time intervals was timely measured by a thermocouple. The whole dynamic shrinking process was recorded by a digital camera equipped on the top of the quartz holder. Several NC5–NC3-α hydrogels with the same α value were measured to obtain statistic data for the thermoresponsive volume change characteristics.

Reversible and Reproducible Thermoresponsive Bending/Unbending Behaviors of NC5–NC3-8.67 Hydrogels: The NC5–NC3-8.67 hydrogel strip was put in a transparent quartz holder with pure water, and placed on a heating stage (TS62, Instec). Before the dynamic bending experiments, the hydrogel strip had been equilibrated at 25 °C for more than 30 min to reach the full swelling state. Then, the temperature was changed from 25 to 40 °C with thermostatic stage system. Once the strip reached to its maximal bending degree, the temperature was changed from 40 °C back to 25 °C rapidly. The heating–cooling cycle was repeated for several times to test the reversibility and reproducibility of the hydrogel strip. The ambient temperature of NC5–NC3-α hydrogel at different time intervals was timely measured by a thermocouple. The whole dynamic bending process was recorded by a digital camera equipped on the top of the quartz holder.

Encapsulation, Capture, and Transportation Behaviors of NC5–NC3-8.67 Hydrogels: The NC5–NC3-8.67 hydrogel sheets were first cut into rectangles or crosses, and put into a petri dish with deionized water. The hydrogel sheets had been equilibrated at 25 °C for more than 30 min to reach the full swelling state. Plastic beads and PTFE pieces are used as target objects for encapsulation. The water temperature in the container was quickly changed from 30 to 45 °C. The ambient temperature of NC5–NC3-8.67 hydrogels at different time intervals was timely measured by a thermocouple. The whole encapsulation process was recorded by a digital camera. Then, a cross-shaped NC5–NC3-8.67 hydrogel was put into a rectangular container, and reached the full swelling state after being equilibrated at 25 °C for more than 30 min. A pearl connected to a string was used as the bait to fish the cross-shaped NC5–NC3-8.67 hydrogel. With increasing the temperature quickly from 30 to 42 °C, the pearl was wrapped by the cross-shaped NC5–NC3-8.67 hydrogel tightly. The ambient temperature of NC5–NC3-8.67 hydrogels at different time intervals was timely measured by a thermocouple. The whole capture process was recorded by the digital camera. Next, a cross-shaped NC5–NC3-8.67 hydrogel was connected to a string with two pieces of thin magnetic sheet. After equilibrated at 20 °C for more than 30 min to reach the full swelling state, the hydrogel was transferred into a heating bath (45 °C) to lift a PTFE block. The hydrogel was then transferred back into a cold bath (20 °C) to release the PTFE block. The whole transportation process was recorded by a digital camera.

Supporting Information

Supporting Information is available from the Wiley Online Library or from the author.

Acknowledgements

The authors gratefully acknowledge support from the National Natural Science Foundation of China (91434202, 21322605), the Program for Changjiang Scholars and Innovative Research Team in University (IRT1163), and State Key Laboratory of Polymer Materials Engineering (sklpme2014-1-01).

Received: February 1, 2015
Revised: March 5, 2015
Published online: April 9, 2015

[1] Z. B. Hu, X. M. Zhang, Y. Li, *Science* **1995**, *269*, 525.
[2] F. Ilmain, T. Tanaka, E. Kokufuta, *Nature* **1991**, *349*, 400.
[3] S. Juodkazis, N. Mukai, R. Wakaki, A. Yamaguchi, S. Matsuo, H. Misawa, *Nature* **2000**, *408*, 178.
[4] A. Suzuki, T. Tanaka, *Nature* **1990**, *346*, 345.
[5] B. P. Lee, S. Konst, *Adv. Mater.* **2014**, *26*, 3415.
[6] K. Lee, S. A. Asher, *J. Am. Chem. Soc.* **2000**, *122*, 9534.
[7] C. X. Ma, T. F. Li, Q. Zhao, X. X. Yang, J. J. Wu, Y. W. Luo, T. Xie, *Adv. Mater.* **2014**, *26*, 5665.
[8] T. S. Shim, S. H. Kim, C. J. Heo, H. C. Jeon, S. M. Yang, *Angew. Chem. Int. Ed.* **2012**, *51*, 1420.
[9] M. R. Islam, X. Li, K. Smyth, M. J. Serpe, *Angew. Chem. Int. Ed.* **2013**, *52*, 10330.
[10] Y. Ma, Y. Y. Zhang, B. S. Wu, W. P. Sun, Z. G. Li, J. Q. Sun, *Angew. Chem. Int. Ed.* **2011**, *50*, 6254.
[11] Y. Ma, J. Q. Sun, *Chem. Mater.* **2009**, *21*, 898.
[12] Z. Liu, L. Liu, X. J. Ju, R. Xie, B. Zhang, L. Y. Chu, *Chem. Commun.* **2011**, *47*, 12283.
[13] P. Mi, X.J. Ju, R. Xie, H.G. Wu, J. Ma, L.Y. Chu, *Polymer* **2010**, *51*, 1648.
[14] T. Tu, W. W. Fang, Z. M. Sun, *Adv. Mater.* **2013**, *25*, 5304.
[15] Z. Xiong, M. L. Zheng, X. Z. Dong, W. Q. Chen, F. Jin, Z. S. Zhao, X. M. Duan, *Soft Matter* **2011**, *7*, 10353.
[16] K. Kajiwara, S. B. Ross-Murphy, *Nature* **1992**, *355*, 208.
[17] Y. Osada, H. Okuzaki, H. Hori, *Nature* **1992**, *355*, 242.
[18] T. Tanaka, I. Nishio, S. T. Sun, S. Ueno-Nishio, *Science* **1982**, *218*, 467.
[19] D. J. Beebe, J. S. Moore, J. M. Bauer, Q. Yu, R. H. Liu, C. Devadoss, B. H. Jo, *Nature* **2000**, *404*, 588.
[20] D. Seliktar, *Science* **2012**, *336*, 1124.
[21] M. A. Stuart, W. S. Huck, J. Genzer, M. Muller, C. Ober, M. Stamm, G. B. Sukhorukov, I. Szleifer, V. V. Tsukruk, M. Urban, F. Winnik, S. Zauscher, I. Luzinov, S. Minko, *Nat. Mater.* **2010**, *9*, 101.
[22] X. M. He, M. Aizenberg, O. Kuksenok, L. D. Zarzar, A. Shastri, A. C. Balazs, J. Aizenberg, *Nature* **2012**, *487*, 214.
[23] E. Kumacheva, *Nat. Mater.* **2012**, *11*, 665.

[24] L. Liu, W. Wang, X. J. Ju, R. Xie, L. Y. Chu, *Soft Matter* **2010**, *6*, 3759.
[25] K. Nagase, J. Kobayashi, T. Okano, *J. R. Soc. Interface* **2009**, *6*, S293.
[26] A. Sidorenko, T. Krupenkin, A. Taylor, P. Fratzl, J. Aizenberg, *Science* **2007**, *315*, 487.
[27] Y. Takashima, S. Hatanaka, M. Otsubo, M. Nakahata, T. Kakuta, A. Hashidzume, H. Yamaguchi, A. Harada, *Nat. Commun.* **2012**, *3*, 1.
[28] P. Calvert, *Adv. Mater.* **2009**, *21*, 743.
[29] W. K. Wang, Z. B. Sun, M. L. Zheng, X. Z. Dong, Z. S. Zhao, X. M. Duan, *J. Phys. Chem. C* **2011**, *115*, 11275.
[30] M. Kondo, Y. L. Yu, T. Ikeda, *Angew. Chem. Int. Ed.* **2006**, *45*, 1378.
[31] L. Ionov, *Mater. Today* **2014**,*17*, 494.
[32] M. Moua, R. R. Kohlmeyer, J. Chen, *Angew. Chem. Int. Ed.* **2013**, *52*, 9234.
[33] V. Magdanz, G. Stoychev, L. Ionov, S. Sanchez, O. G. Schmidt, *Angew. Chem. Int. Ed.* **2014**, *53*, 2673.
[34] S. Pedron, S. van Lierop, P. Horstman, R. Penterman, D. J. Broer, E. Peeters, *Adv. Funct. Mater.* **2011**, *21*, 1624.
[35] P. Techawanitchai, M. Ebara, N. Idota, T. A. Asoh, A. Kikuchi, T. Aoyagi, *Soft Matter* **2012**, *8*, 2844.
[36] H. Y. He, J. J. Guan, J. L. Lee, *J. Controlled Release* **2006**, *110*, 339.
[37] K. E. Laflin, C. J. Morris, N. Bassik, M. Jamal, D. H. Gracias, *J. Microelectromech. Syst.* **2011**, *20*, 505.
[38] T. G. Leong, C. L. Randall, B. R. Benson, N. Bassik, G. M. Stern, D. H. Gracias, *Proc. Natl. Acad. Sci. U.S.A.* **2009**, *106*, 703.
[39] E. Z. Zhang, T. Wang, W. Hong, W. X. Sun, X. X. Liu, Z. Tong, *J. Mater. Chem. A* **2014**, *2*, 15633.
[40] D. Morales, E. Palleau, M. D. Dickey, O. D. Velev, *Soft Matter* **2014**, *10*, 1337.
[41] J. Kim, J. A. Hanna, R. C. Hayward, C. D. Santangelo, *Soft Matter* **2012**, *8*, 2375.
[42] H. Therien-Aubin, Z. L. Wu, Z. H. Nie, E. Kumacheva, *J. Am. Chem. Soc.* **2013**, *135*, 4834.
[43] M. Byun, C. D. Santangelo, R. C. Hayward, *Soft Matter* **2013**, *9*, 8264.
[44] T. A. Asoh, M. Matsusaki, T. Kaneko, M. Akashi, *Adv. Mater.* **2008**, *20*, 2080.
[45] G. Stoychev, N. Puretskiy, L. Ionov, *Soft Matter* **2011**, *7*, 3277.
[46] V. Stroganov, S. Zakharchenko, E. Sperling, A. K. Meyer, O. G. Schmidt, L. Ionov, *Adv. Funct. Mater.* **2014**, *24*, 4357.
[47] S. Zakharchenko, N. Puretskiy, G. Stoychev, M. Stamm, L. Ionov, *Soft Matter* **2010**, *6*, 2633.
[48] J. J. Zhang, J. J. Wu, J. Z. Sun, Q. Y. Zhou, *Soft Matter* **2012**, *8*, 5750.
[49] J. P. Gong, *Soft Matter* **2010**, *6*, 2583.
[50] J. Y. Sun, X. H. Zhao, W. R. K. Illeperuma, O. Chaudhuri, K. H. Oh, D. J. Mooney, J. J. Vlassak, Z. G. Suo, *Nature* **2012**, *489*, 133.
[51] K. Haraguchi, H. J. Li, *Angew. Chem. Int. Ed.* **2005**, *44*, 6500.
[52] K. Haraguchi, T. Takada, *Macromolecules* **2010**, *43*, 4294.
[53] K. Haraguchi, T. Takehisa, *Adv. Mater.* **2002**, *14*, 1120.
[54] K. Haraguchi, T. Takehisa, S. M. Fan, *Macromolecules* **2002**, *35*, 10162.
[55] K. Haraguchi, S. Taniguchi, T. Takehisa, *ChemPhysChem* **2005**, *6*, 238.
[56] H. W. Kang, Y. Tabata, Y. Ikada, *Biomaterials* **1999**, *20*, 1339
[57] L. W. Xia, R. Xie, X. J. Ju, W. Wang, Q. Chen, L. Y. Chu, *Nat. Commun.* **2013**, *4*, 2226.